Large band MEMS microphone for high frequency acoustic applications in air

L. Rufer[a], A. Koumela[a], Z. Zhou[b], M. Wong[b], S. Ollivier[c], E. Salze[c], P. Yuldashev[d], S. Basrour[a] et P. Blanc-Benon[c]

[a]Univ. Grenoble Alpes, TIMA, F-38031 Grenoble, CNRS, TIMA, F-38031 Grenoble, France

[b]Hong Kong University of Science and Technology, Department of Electronic and Computer Engineering, – Hong Kong, Chine

[c]LMFA, Ecole Centrale de Lyon, 36 avenue Guy de Collongue, 69134 Ecully, France

[d]Moscow State University, Department of General Physics and Condensed Matter Physics, Faculty of Physics, Moscow State University, 119991 Moscou, Fédération de Russie

alexandra.koumela@imag.fr

In this paper, we present a test bench for the acoustic characterization of high frequency large band microphones. An interferometry optical method is used for the calibration of the N-waves and the extraction of the pressure sensed by the microphones. Moreover, we compare the experimental results obtained from two different MEMS architectures. It is shown, that the optimization of the damping leads to better results reducing parasitic oscillations on the microphone response. The optimized microphone has a useful frequency band of 400kHz and the sensitivity achieved in a flat low-frequency part of its frequency characteristics is 0.66 µV/V/Pa.

1 Introduction

In the last decade, MEMS-based microphones have reached the maturity and became a part of many mobile devices. There was also announced a measuring MEMS-based microphone having a good uniformity on sensitivity and frequency response and reaching the noise level of 23 dB(A), which is 7 dB lower than state-of-the-art 1/4-inch measurement microphones [1]. Most of these devices require sensors covering entirely or partially the audible frequency range. There are other applications requiring acoustic sensors of air-borne sound exceeding considerably a high-frequency limit of standard measuring microphones. These sensors are actually not available off-the-shelf. Industries such as high-speed train, supersonic aviation and defense demand a development of advanced aero-acoustic measuring tools [2]-[4]. Microphones with large-band characteristics (10 kHz – 1 MHz) and a dynamic range from 40 Pa to 4 kPa are needed to characterize ultrasonic wave generation and propagation associated with acoustic scaled models used in research and development tasks [5].

The technological progress in the domain of MEMS (Micro Electro Mechanical Systems) devices enables nowadays the design and fabrication of microphones with extended frequency range. We have demonstrated recently, a piezoresistive microphone with a sensing diaphragm released from its backside using a bulk micro-fabrication process [6]. Comparing to our previous designs, the advantage of the backside release consists in the absence of releasing holes on the diaphragm and thus the absence of acoustic "short-circuit".

Previous communications were focused on the fabrication aspects and the validation of the microphone design. In this paper, we will detail the characterization procedure, the test conditions and we will show the experimental results obtained.

2 Microphone design

In a first step, we have designed a piezoresistive MEMS microphone with a structure consisting of a fully clamped squared low stress SiN (LS-SiN) diaphragm suspended over a cavity. As sensing elements there are used four polysilicon piezoresistors that are positioned at the middle of the four diaphragm edges as shown in Figure 1(a). There is also a reference resistor next to each piezoresistor and all of them are connected to form a Wheatstone bridge (Figure 2). In fact, each resistive element (noted 2R or $2R+\Delta R_{Di}$ in Figure 2) of the bridge corresponds to two grouped resistive elements (resistances or piezoresistances) on the diaphragm design. We have developed several devices having the diaphragm size in a range from 150x150 μm^2 to 300x300 μm^2. However, due to the necessity of a trade-off between high resonant frequency and sensitivity, we will present here only the results for the diaphragm measuring 300x300 μm^2. An optical photograph (top-view) of the diaphragm with piezoresistors is shown in Figure 1(a), while a schematic cross-section of the device is shown in Figure 1(b). It can be noticed that the backside of the silicon chip is entirely etched.

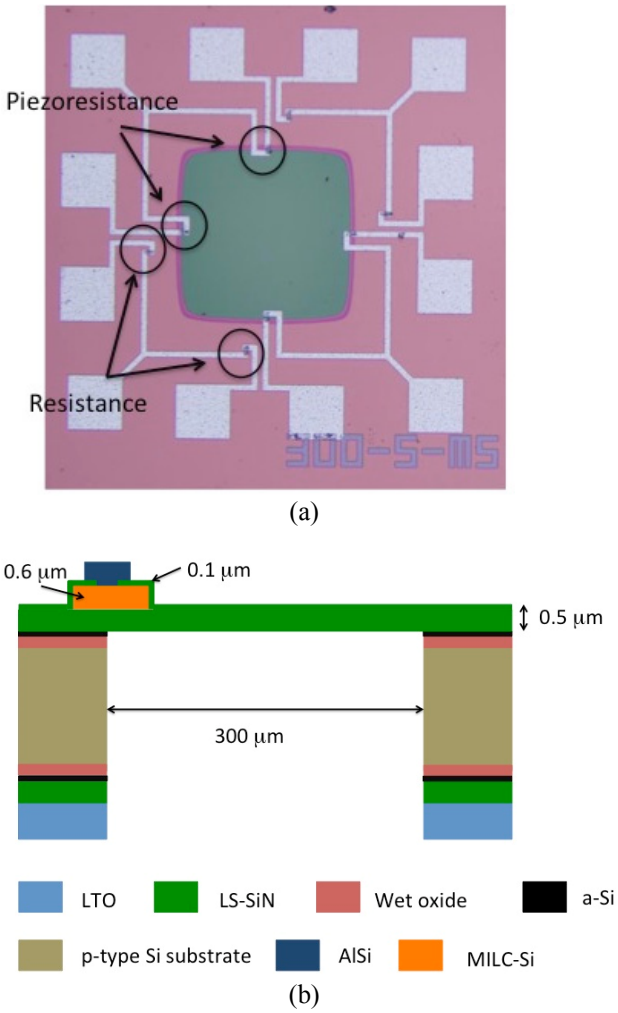

Figure 1. The piezoresistive microphone without back-plate: a) Optical photograph (top-view); b) Schematic cross-section of the device. The thickness of the SiN diaphragm is 0.5 µm.

This rather simple structure of the microphone, having a diaphragm damped only with its internal stress and acoustic radiation effect, has shown strong oscillations degrading the microphone response.

For this reason, we decided to improve the original design by implementing an additional viscous damping. The viscous damping is introduced by means of a perforated damping plate located underneath the sensing diaphragm. In this design, due to fabrications issues, the diaphragm is no longer flat and has on its inner side protrusions corresponding to each perforation hole as shown in detail in Figure 3. The resulting value of the damping coefficient is composed of contributions corresponding to the squeezed-film effect in the air-gap, to

the damping caused by air-flow through a vertical annular flow-channel in the perforation, and to damping caused by the sliding protrusion of the diaphragm in the perforation.

An optical photograph of the improved microphone is shown in Figure 4(a). The holes that one can observe by transparency of the LS-SiN membrane correspond to the perforation of the damping plate. Figure 4(b) shows the schematic cross-section of the device. The damping plate made of LS-SiN, is 2 µm thick. The microphone diaphragm is in both designs 0.5 µm thick, while the gap between the diaphragm and the damping plate in the second design is also 0.5 µm.

The fabrication process is described more in detail for each design in [6] and [7].

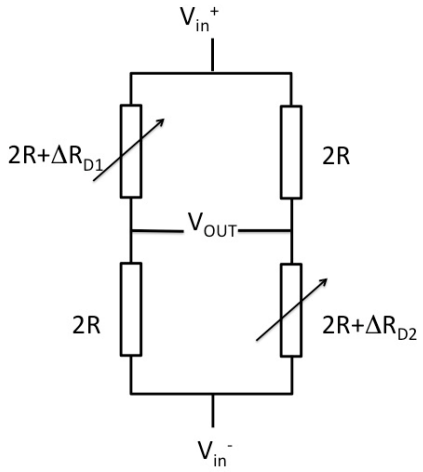

Figure 2. Wheatstone bridge. Each resistive element of the bridge corresponds to two polysilicon resistances on the microphone design.

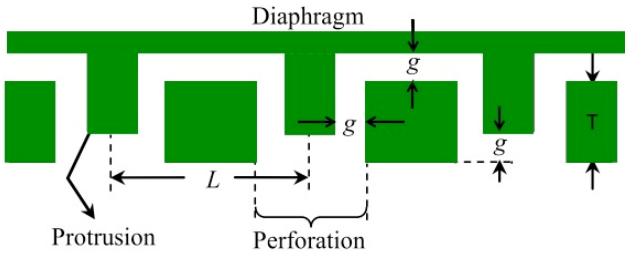

Figure 3. Detail of the schematic cross-section for the improved microphone. The period L of the structure is 10 µm, the gap g is 0.5 µm and the thickness of the back-plate T is 2 µm.

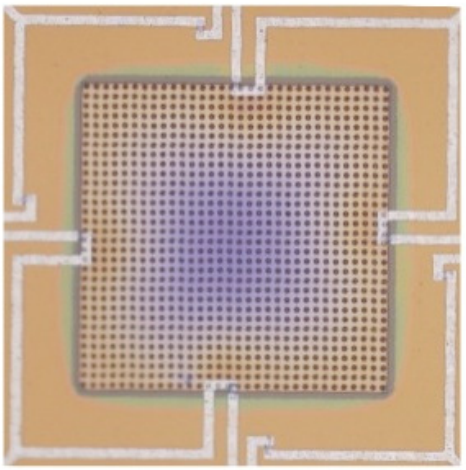

(a)

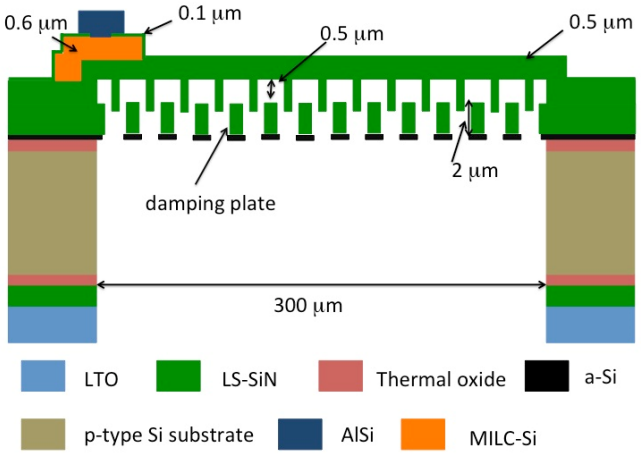

(b)

Figure 4. The piezoresistive microphone with back-plate: a) Optical photograph (top-view); b) Schematic cross-section of the device

3 Test set-up

The acoustic characterization of the microphones was performed with calibrated N-waves generated by a spark source. As shown in Figure 5, electrical sparks are obtained by discharging a capacitor ($C \approx 1$ nF) that is continuously charged through a resistor ($R \approx 100$ MΩ) from a high-voltage source ($V \approx 14 - 16$ kV). The capacitor is discharged through a pair of electrodes fixed at a mutual distance of 20 mm. The electrical discharge is accompanied with electromagnetic, optical and acoustic effects.

The acoustic effect in a form of N-wave can be exactly predicted and can be also calibrated with a high accuracy by using an optical interferometry method. More details of the method can be found in [8]. In Figure 6(a), two of the optical elements in front of the microphone set-up are shown. In fact, between these two lenses, there is a laser beam which is disturbed every time a shock-wave passes through. This results in a change of the optical path of the beam that is compared to a similar non-disturbed optical path. The interference between these two beams gives us information about the sound wave that reaches the microphone.

In order to perform the measurement, we mounted the microphone on a PCB card (shown in Figure 6(b)). The two inputs of the Wheatstone bridge are polarized at ±1.5 V

while the output is connected at the input of a differential instrumentation amplifier (gain ≈ 1000) for the amplification of the microphone signal. The amplified output is then monitored and registered with an oscilloscope. The electronics are placed inside a shielding box in order to protect them from the electromagnetic component of the discharge.

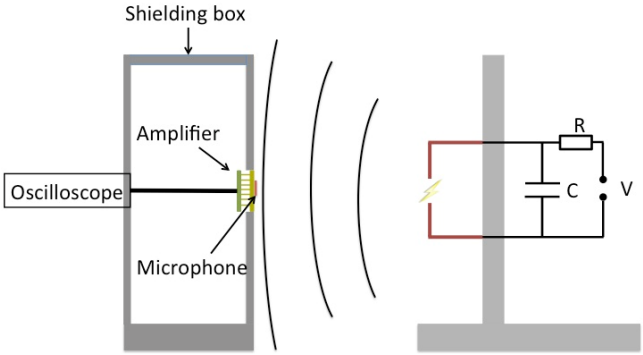

Figure 5. Schematic diagram of the microphone calibration setup: Right - Spark source used for the generation of acoustic N-waves; Left – Microphone under calibration in the shielding box.

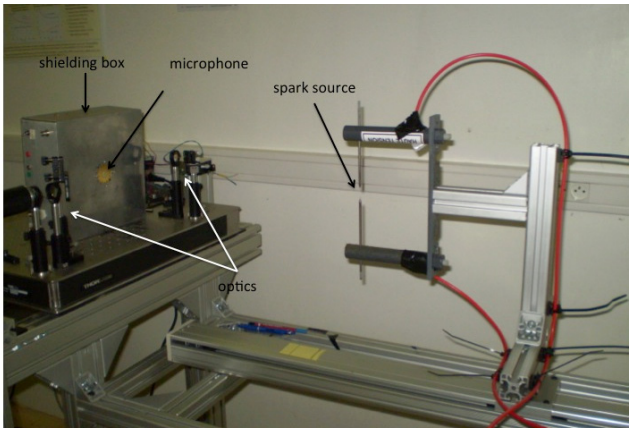

(a)

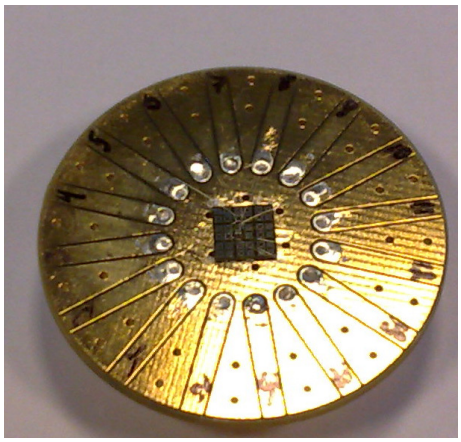

(b)

Figure 6. (a) Photograph of the test bench with the spark source, the shielding box and the microphone. Also, a part of the optics used to detect the sound wave and calibrate it is shown on the figure. (b) The PCB card used to mount the samples with a bonded silicon chip on it.

4 Microphone characterization

Measurements were performed with both microphone designs. The dimensions of the diaphragm in both designs were the same: 300 x 300 um^2. In Figure 7, the output voltage of the Wheatstone bridge for the first generation microphone is shown along with an ideal N-wave. We can distinguish the 'N' form of the wave measured with the microphone, however we observe also unwanted oscillations. We can estimate, from the oscillations period in Figure 7, the microphone resonant frequency of 357 kHz. The high oscillation amplitude of the microphone diaphragm indicates a high quality factor of the sensor, which is not compatible with the application. In Figure 8, the normalized spectrum of both the microphone and the ideal N-wave are shown in the frequency domain. The single-sided spectra were obtained by applying the Fourier transform to the time-domain signals in Figure 7. The microphone mechanical resonance at 342 kHz is visible.

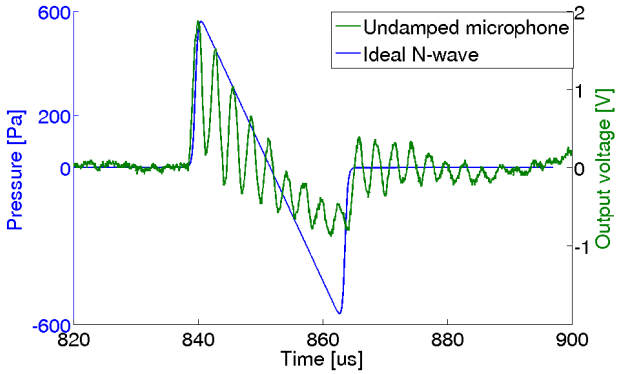

Figure 7. Un-damped microphone. Ideal N-wave (in blue) giving estimation for the acoustic pressure of the sound wave and the microphone output (in green) in the time domain.

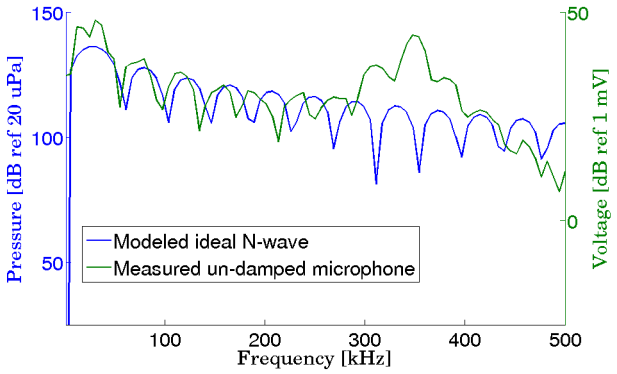

Figure 8. Comparison of the un-damped microphone spectrum with the ideal N-wave spectrum in the frequency domain. The resonant frequency of the microphone is well pronounced.

In Figure 9, we have plotted the output in the time domain of the damped microphone. In this case, the microphone response is plotted along with the reference measurement obtained with the laser interferometry technique. The improvement that the new microphone design offered to the quality of the output signal is obvious when comparing Figure 7 and Figure 9. In the case of the damped microphone, the oscillations of the diaphragm are no more visible, meaning that the mechanical resonance is much attenuated. Similarly with the un-damped device, we

plotted the normalized spectra of the damped microphone along with the laser calibration results in Figure 10. Here too, the mechanical resonance of the diaphragm is clearly attenuated with respect to the spectrum of the un-damped device shown in Figure 8.

The sensitivity of the improved microphone was obtained by dividing the microphone results by the laser output (Figure 11). We can also calculate the sensitivity of the damped device directly from the time domain response in Figure 9. Dividing the minimum of the microphone output voltage by the minimum of the pressure and by the input voltage of the Wheatstone bridge, we obtain a sensitivity of 0.66 µV/V/Pa.

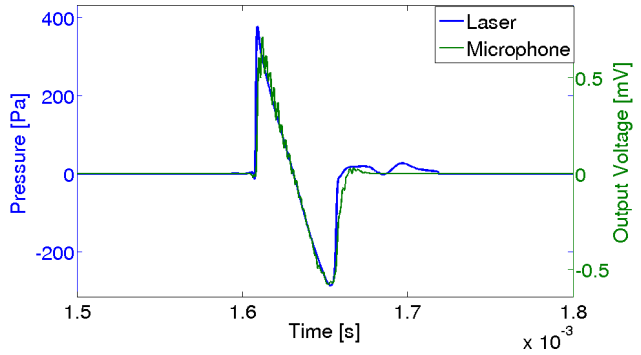

Figure 9. Measurement result on the improved (damped) microphone in the time domain: Optical measurement (in blue) giving the pressure of the sound wave and the microphone output (in green).

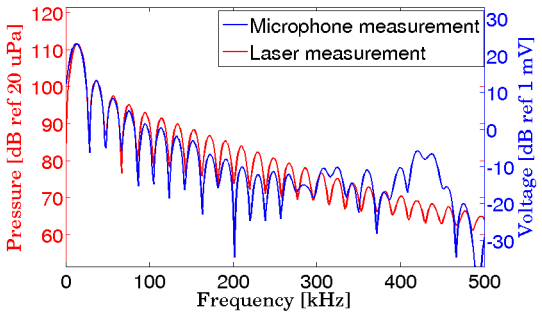

Figure 10. Frequency spectra of the acoustic pressure obtained from the damped microphone response and from the optical calibration.

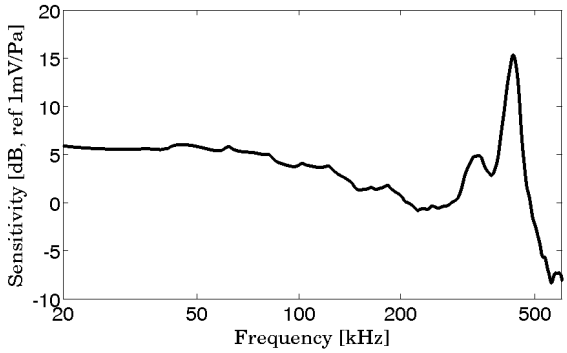

Figure 11. Electrical sensitivity of the damped microphone at 3 V dc bias and 60 dB amplifier gain.

5 Conclusion

We presented a test bench for the acoustic characterization of high-frequency microphones. A novel calibration method based on an optical interferometry technique was used in order to extract information about the sound wave pressure to be compared with microphone measurements. Moreover, we showed the results for two different architectures of MEMS microphones and we have reported the importance of an optimal structure damping. The damped microphone has a useful frequency band of 400 kHz and in its low frequency part shows the sensitivity of 0.66 µV/V/Pa.

Acknowledgements

This work has been done with the support of the French National Research Agency (ANR) Program BLANC 2010 SIMI 9 for the project SIMMIC and within the framework of the Labex CeLyA of Université de Lyon, operated by the French National Research Agency (ANR-10-LABX-0060/ ANR-11-IDEX-0007).

References

[1] P.R. Scheeper, B. Nordstrand, J.O. Gullv, Bin Liu, T. Clausen, L. Midjord, T. Storgaard-Larsen, "A new measurement microphone based on MEMS technology", Journal of Microelectromechanical Systems, Vol.12, No. 6, pp. 880 – 891.

[2] S. Oerlemans, L. Broersma, and P. Sijtsma, "Quantification of airframe noise using microphone arrays in open and closed wind tunnels," National Aerospace Laboratory NLR, Report, 2007.

[3] M. Remillieux, "Aeroacoustic Study of a Model-Scale Landing Gear in a Semi-Anechoic Wind-Tunnel," MSc Thesis, Department of Mechanical Engineering, Virginia Polytechnic Institute and State University, 2007.

[4] A. Bale, "The Application of MEMS Microphone Arrays to Aeroacoustic Measurements, MASc Thesis, Department of Mechanical Engineering, University of Waterloo, 2011.

[5] M. Averiyanov, "Nonlinear-diffraction effects in propagation of sound waves through turbulent atmosphere: Experimental and theoretical studies," Ph.D. dissertation, École Centrale de Lyon, Écully, France, 2008.

[6] Z. Zhou, L. Rufer, E. Salze, S. Ollivier and M. Wong, 'Wide-band aero-acoustic microphone with improved low-frequency characteristics', Transducers 2013, 16-20 June 2013.

[7] Z. Zhou, L. Rufer and M. Wong, 'Damped Aero-Acoustic Microphone with Improved High- Frequency Characteristics', Journal of Microelectromechanical Systems, 99.

[8] S. Ollivier, E. Salze, C. Desjouy, P. V. Yuldashev, V. Khokhlova and P. Blanc-Benon, 'Méthodes de calibration des microphones en hautes fréquences (10kHz-1 MHz)', Proceedings CFA 2014, Poitiers.